Parasitology International 66 (2017) 227–235

Contents lists available at ScienceDirect

Parasitology International

journal homepage: www.elsevier.com/locate/parint

Activation and exhaustion of antigen-specific CD8$^+$ T cells occur in different splenic compartments during infection with *Plasmodium berghei*

Ganchimeg Bayarsaikhan [a,b], Mana Miyakoda [a], Kazuo Yamamoto [c], Daisuke Kimura [a], Masoud Akbari [a], Masao Yuda [d], Katsuyuki Yui [a,b,*]

[a] Division of Immunology, Department of Molecular Microbiology and Immunology, Graduate School of Biomedical Sciences, Nagasaki University, 1-12-4, Sakamoto, Nagasaki 852-8523, Japan
[b] Program for Nurturing Global Leaders in Tropical and Emerging Infectious Diseases, Graduate School of Biomedical Sciences, Nagasaki University, 1-12-4, Sakamoto, Nagasaki 852-8523, Japan
[c] Division of Cell Function Research Support, Biomedical Research Support Center, School of Medicine, Nagasaki University, 1-12-4, Sakamoto, Nagasaki 852-8523, Japan
[d] Department of Medical Zoology, School of Medicine, Mie University, 2-174, Edobashi, Tsu 514-8507, Japan

ARTICLE INFO

Article history:
Received 29 September 2016
Received in revised form 12 December 2016
Accepted 16 January 2017
Available online 03 February 2017

Keywords:
CD8$^+$ T cells
Infectious diseases
Inhibitory receptors
Malaria
Spleen

ABSTRACT

The spleen is the major organ in which T cells are primed during infection with malaria parasites. However, little is known regarding the dynamics of the immune responses and their localization within the splenic tissue during malaria infection. We examined murine CD8$^+$ T cell responses during infection with *Plasmodium berghei* using recombinant parasites expressing a model antigen ovalbumin (OVA) protein and compared the responses with those elicited by *Listeria monocytogenes* expressing the same antigen. OVA-specific CD8$^+$ T cells were mainly activated in the white pulp of the spleen during malaria infection, as similarly observed during Listeria infection. However, the fates of these activated CD8$^+$ T cells were distinct. During infection with malaria parasites, activated CD8$^+$ T cells preferentially accumulated in the red pulp and/or marginal zone, where cytokine production of OVA-specific CD8$^+$ T cells decreased, and the expression of multiple inhibitory receptors increased. These cells preferentially underwent apoptosis, suggesting that T cell exhaustion mainly occurred in the red pulp and/or marginal zone. However, during Listeria infection, OVA-specific CD8$^+$ T cells only transiently expressed inhibitory receptors in the white pulp and maintained their ability to produce cytokines and become memory cells. These results highlighted the distinct fates of CD8$^+$ T cells during infection with *Plasmodium* parasites and Listeria, and suggested that activation and exhaustion of specific CD8$^+$ T cells occurred in distinct spleen compartments during infection with malaria parasites.

1. Introduction

Malaria, caused by infection with *Plasmodium* species parasites, is one of the most prevalent infectious diseases in the world [1]. During the blood-stage of *Plasmodium* infection, both CD4$^+$ and CD8$^+$ T cells are activated and these T cells play critical roles in both malaria pathogenesis and protection against malaria. CD4$^+$ T cells help B cells produce anti-parasite antibodies, activate macrophages to engulf parasites, and play pivotal roles in protecting against parasites [2,3]. CD8$^+$ T cells play major roles in malaria pathogenesis, as observed with experimental cerebral malaria [4,5]. These parasite-specific CD8$^+$ T cells were generated by transporter of antigen presentation (TAP)-dependent cross-presentation of malaria antigens by CD8α$^+$ dendritic cells (DCs) during blood-stage infection [6,7]. Effector CD8$^+$ T cells also appeared to play protective roles against the blood-stage of malaria infection, as shown by the transfer of protective immunity by CD8$^+$ T cells from the repeatedly immunized mice [8]. However, CD8$^+$ T cells that are activated by infection with malaria parasites express multiple inhibitory molecules, including programmed cell death protein-1 (PD-1) and lymphocyte activated gene-3 (LAG-3), and are functionally disabled during chronic infection, reflecting a state of exhaustion [9,10]. In a model of experimental cerebral malaria, it was also shown that the activation and pathogenesis of T cells were inhibited by PD-1 in resistant BALB/c mice during acute infection with *P. berghei* ANKA, although T cells exhibited pathogenesis in susceptible C57BL/6 stain despite high levels of PD-1 expression [11].

Abbreviations: CFSE, 5-(and 6)-carboxyfluorescein diacetate succinimidyl ester; DCs, dendritic cells; LAG-3, lymphocyte activated gene 3; LCMV, lymphocytic choriomeningitis virus; LM-OVA, *Listeria monocytogenes* expressing OVA; mAb, monoclonal antibody; MFI, mean fluorescent intensity; MMM, marginal zone metallophilic macrophages; MZ, marginal zone; MZM, marginal zone macrophages; OVA, ovalbumin; PbA-OVA, *Plasmodium berghei* ANKA expressing OVA; PD-1, programmed cell death protein; RBCs, red blood cells; RP, red pulp; SLEC, short-lived effector; TIM-3, T-cell immunoglobulin and mucin-domain containing-3; WP, white pulp.

* Corresponding author at: Division of Immunology, Department of Molecular Microbiology and Immunology, Graduate School of Biomedical Sciences, 1-12-4, Sakamoto 852-8523, Japan.
E-mail address: katsu@nagasaki-u.ac.jp (K. Yui).

http://dx.doi.org/10.1016/j.parint.2017.01.022
1383-5769/

The spleen is the main organ to filter red blood cells (RBCs) and elicits immune responses to blood-borne pathogens [12]. It is composed of 3 main compartments, the white pulp (WP), where most T and B cells resides and immune responses are initiated, the red pulp (RP), where RBCs are filtered, and the marginal zone (MZ) that separates the WP and RP and contains MZ B cells and macrophages [12]. The MZ is the site of antigen trapping in the spleen and contains 2 types of macrophages; MZ metallophilic macrophages (MMMs), which are located in the inner MZ near the WP, and MZ macrophages (MZMs) localized in the outer MZ towards the RP [13,14]. $CD8^+$ T-cell responses in the spleen have been characterized using infection models with microbes, including intracellular bacterium *Listeria monocytogenes* and lymphocytic choriomeningitis virus (LCMV). The spleen contains 2 main DC subsets, $CD8\alpha^+$ DCs, which reside mainly in the T cell zone, and $CD8\alpha^-$ DCs, which are localized primarily in the RP and MZ [15,16]. $CD8\alpha^+$ DCs are directly infected with *L. monocytogenes* or capture microbial antigens, after which they can move from the MZ to enter the WP, where they present antigens to $CD8\alpha^+$ T cells [17–19]. The initial activation of antigen-specific $CD8^+$ T cells occurs at the borders of the B and T cell zones in the WP, followed by cluster formation with DCs in the WP [20]. After activation, these $CD8^+$ T cells proliferate, forming effector and memory cells, and exit to the RP through bridging channels. Studies using the LCMV model showed that memory precursor cells mainly localized in the T cell zone of the WP, whereas terminal effector cells localized exclusively to the RP of the spleen. Upon re-challenge, memory or memory precursor $CD8^+$ T cells expand and are redistributed in the RP [21–23].

Results from previous studies showed the dynamics of splenic lymphocyte responses during infection with *Plasmodium* parasites [24,25]. Furthermore, the spleen architecture is altered, and MZMs and MMMs are both lost during infection with *P. chabaudi*, with the loss of MMMs being dependent on $CD8^+$ T cells [26]. However, the localization and dynamics of antigen-specific $CD8^+$ T cells in the spleen during malaria infection are not clearly understood. The model antigen ovalbumin (OVA) protein has been used to study antigen-specific immune responses during infection with recombinant pathogen expressing OVA, such as *L. monocytogenes* expressing OVA (LM-OVA) and T-cell receptor-transgenic OT-1 mice [20]. We developed a model of $CD8^+$ T cell activation during malaria infection using *Plasmodium berghei* ANKA that express OVA (PbA-OVA) [6]. In this study, we used this model system to study specific $CD8^+$ T-cell responses in different splenic tissue compartments. Using OVA as a common model antigen, we compared the responses of specific $CD8^+$ T cells during infection with *Plasmodium* parasites and Listeria.

2. Materials and methods

2.1. Mice

OT-I transgenic mice expressing the T cell receptor specific for $OVA_{257–264}/K^b$ were provided by Dr. H. Kosaka (Osaka University, Osaka, Japan) [27]. C57BL/6 mice were purchased from SLC (Shizuoka, Japan). B6.SJL and OT-I mice were bred, and the offspring were intercrossed to obtain $CD45.1^+$ OT-I mice. Mice were maintained in the Laboratory Animal Center for Animal Research at Nagasaki University, and both male and female mice were used at 7–10 weeks of age. The animal experiments were approved by the Institutional Animal Care and Use Committee of Nagasaki University and were conducted according to the guidelines for Animal Experimentation of Nagasaki University.

2.2. Infections and adoptive transfer

The recombinant parasite PbA-OVA, which constitutively expresses OVA under the control of the hsp70 promotor, was maintained as described previously [6]. Mice were infected with RBCs (5×10^4) infected with PbA-OVA or PbA by intraperitoneal injection. LM-OVA [28] was provided by Dr. Y. Yoshikai (Kyushu University) and Dr. H. Shen (University of Pennsylvania). Mice were infected with LM-OVA (10^6 colony-forming units, 0.1 LD_{50}) by intraperitoneal injection. $CD8^+$ (>95%) were prepared from the spleen, brachial, and inguinal lymph nodes using *anti*-CD8 IMag (BD Biosciences, San Diego, CA, USA) and labeled with CFSE (15 μM, Molecular Probes), as described previously [6]. C57BL/6 mice were adoptively transferred intravenously (i.v.) with $CD8^+$ OT-I cells (1×10^6) prepared from age- and sex-matched OT-I mice and were infected with PbA-OVA or LM-OVA on the following day.

2.3. Immunohistochemistry

Spleen tissues were prepared for immunohistochemistry, as previously described [29]. Briefly, fresh frozen spleens were embedded in Tissue-Tek OCT compound (Sakura Finetek, Tokyo, Japan), cut into 5-μm sections with a cryomicrotome, and fixed with acetone for 15 min at room temperature. Samples were blocked by Blocking One Histo (Nacalai, Kyoto, Japan) for 1 h in a humid chamber at room temperature. Sections were stained for CD45.1 and CD169 (BioLegend, San Diego, CA, USA) overnight at 4 °C and mounted in DAKO fluorescent mounting medium (Agilent Technologies, Santa Clara, CA, USA). Images were acquired by fluorescence microscopy (Olympus, Tokyo, Japan) and merged using ImageJ software (National Institutes of Health, Bethesda, MD, USA). The number of OT-I cells was counted in a 0.5-mm^2 area in a microscopic field using ImageJ software. Statistical analysis was performed on 15 different areas from 1 spleen, and 3 different mice were examined.

2.4. Flow cytometry

To stain cells in the RP, mice received PE-*anti*-CD8α mAb (3 μg, clone 53–6.7) via i.v. injection and were euthanized 3 min later, as previously described [30]. The spleens were harvested, and RBCs were lysed using Gey's solution. Lymphocytes were stained with mAbs or their isotype controls. All mAbs were purchased from eBioscience (San Diego, CA, USA), BioLegend, BD Pharmingen (Franklin Lakes, NJ, USA), or Tonbo (San Diego, CA, USA). Staining for annexin V was performed in annexin V binding buffer composed of HEPES (100 mM), $CaCl_2$ (25 mM), and NaCl (1.4 M, pH 7.5), according to the manufacturer's instructions (Sigma-Aldrich, St. Louis, MO, USA). The compound 7-aminoactinomycin D (7AAD) was added to exclude dead cells from the analysis. For intracellular staining, $CD8^+$ T cells were purified using magnetic-activated cell sorting (MACS) microbeads and AutoMACS (Miltenyi Biotec, Gladbach, Germany) and were stimulated for 4 h with DCs (3×10^4) pulsed with the $OVA_{257–264}$ peptide (1 μg/mL) in 24-well plates. Cells were stained for the appropriate surface markers, fixed, permeabilized using Cytofix/Cytoperm buffer (BD Bioscience), stained with *anti*-cytokine mAbs, and analyzed using a FACS Canto II instrument (BD Biosciences). The number of cellular subsets was determined by multiplying the total number of spleen cells by the proportion of each subset in the spleen, as determined by flow cytometry.

2.5. Statistical analysis

Results are shown as the mean ± standard deviations (SD). Data were analyzed using GraphPad Prism software, version 6 (GraphPad, San Diego, CA, USA). An overall difference between groups was determined by 2-way analysis of variance (ANOVA). If the 2-way ANOVA revealed a significant difference, then differences between individual groups were estimated using the Tukey's multiple comparison test. $p < 0.05$ was considered significant.

3. Results

3.1. Distribution of OT-I cells in the spleen after infection with PbA-OVA or LM-OVA

To examine the tissue distribution of antigen-specific $CD8^+$ T cells in the spleen during malaria infection, we adoptively transferred C57BL/6 mice with $CD8^+$ T cells from OT-I mice, infected them with PbA-OVA or PbA, and compared the localization of OT-I cells in the splenic compartments with that in mice infected with LM-OVA. Every 2 days after infection, spleen cryosections were prepared and stained with an *anti*-CD169 monoclonal antibody (mAb) that bound MMMs, which were localized in the MZ adjacent to WP border (Fig. 1A). The inner border of CD169 staining was considered a margin between the WP and RP/MZ. In naïve mice, the area size of the WP was approximately half that of the RP/MZ, and OT-I cells distributed in both the WP (approximately 60%) and RP/MZ (approximately 40%). The size of the WP increased 6 days after infection with PbA-OVA and occupied approximately 60% of the splenic section. The distribution of OT-I cells in the WP and RP/MZ was similar to that in naïve mice for up to 4 days after infection with PbA-OVA and increased 6 days after infection in both compartments, in parallel with an increase in parasitemia levels (Fig. 1A upper panel and B). The proportions of OT-I cells within the $CD8^+$ T cell population in mice 6 days after infection with PbA-OVA or PbA were 10.1 ± 3.3 and 0.7 ± 0.1%, respectively, indicating the antigen-specific expansion of OT-I cells in PbA-OVA-infected mice. At 8 days post-infection, CD169 staining weakened, suggestive of a loss of MMMs as previously reported during infection with *P. chabaudi* (Fig. 1A) [26]. Because C57BL/6 mice develop cerebral malaria and die 7–9 days after infection with PbA-OVA, we were unable to observe infected mice beyond 8 days post-infection. In mice infected with LM-OVA, the OT-I cells expanded much more robustly than in mice infected with PbA-OVA infection, consistent with previous data [18,31]. OT-I cells began to expand in the WP at 2 days after infection and their distribution was more pronounced in the RP/MZ than in the WP at 4 days after infection (Fig. 1C). The size of the WP slightly increased, occupying approximately 50% of the section on day 6, which decreased to approximately 40% on day 8. No loss of MMMs was observed during infection with LM-OVA (Fig. 1A).

To characterize cells in different compartments of the spleen in more detail, we stained $CD8^+$ T cells in vivo by intravenous injection with a phycoerythrin (PE)-conjugated, *anti*-CD8α mAb 3 min prior to euthanasia (Fig. 2A) [30]. Because conventional $CD8^+$ T cells express a CD8α–CD8β dimer, binding of an *anti*-CD8α mAb does not hinder staining with an anti-CD8β mAb. The injected mAb reached the RP/MZ, but not the WP, enabling us to distinguish $CD8^+$ T cells that were distributed to these 2 compartments (Fig. 2B). In naïve mice, the proportions of

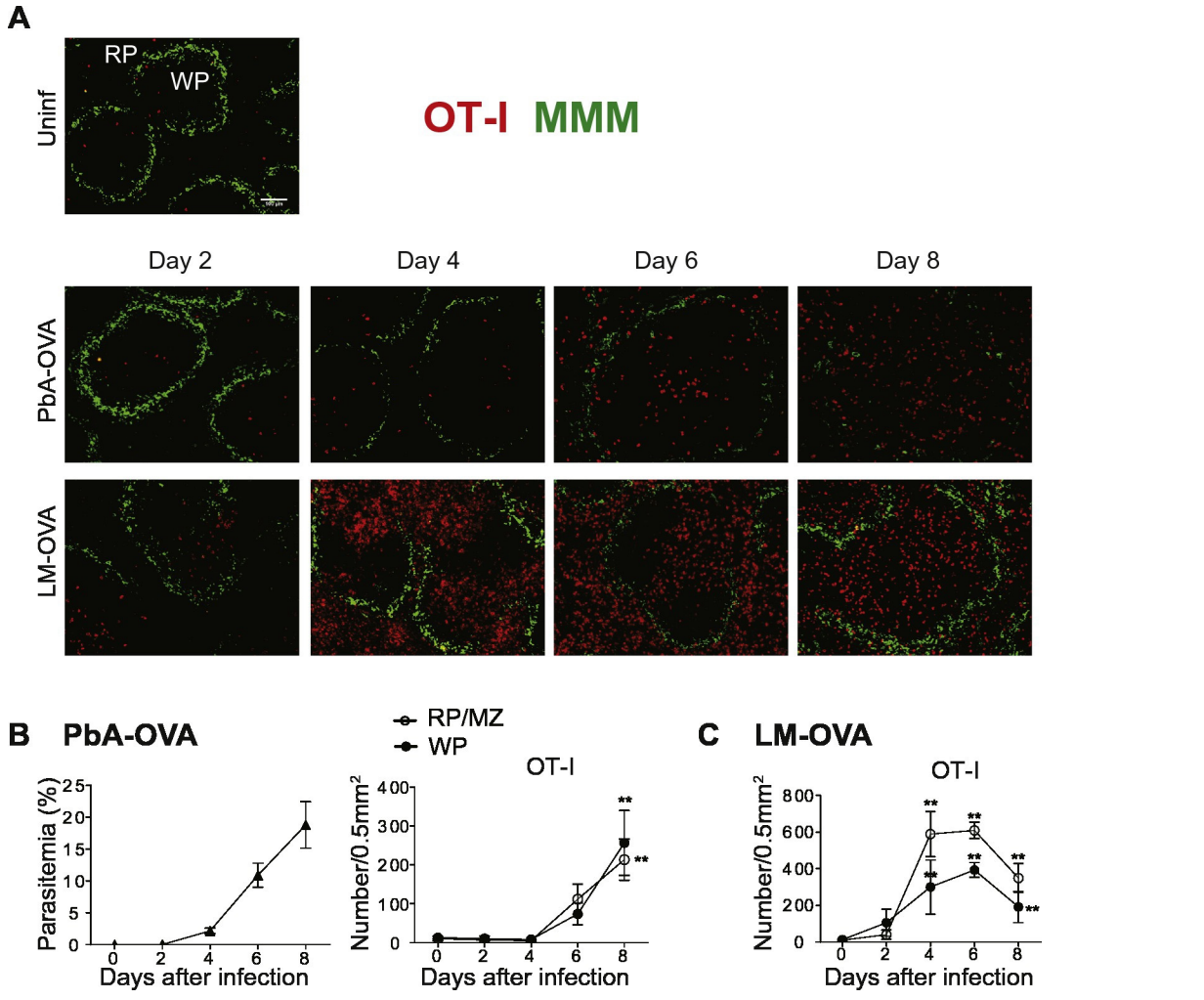

Fig. 1. Distribution of OT-I cells in the spleen of mice infected with PbA-OVA or LM-OVA. C57BL/6 mice were adoptively transferred with OT-I T cells ($CD45.1^+$) and were infected with PbA-OVA (A, B) or LM-OVA (A, C). The spleen sections were stained for CD45.1 (for OT-I cells) and CD169 (for MMMs) and analyzed by fluorescence microscopy (10×) (A). Scale bar, 100 μm. (B, C) Graphs showing the levels of parasitemia (triangles) (B), the number of OT-I cells in the RP/MZ (open circles) and the WP (closed circles) of the spleen after infection with PbA-OVA (B) or LM-OVA (C). The numbers of OT-I cells/0.5-mm^2 area of the spleen were counted on the indicated days post-infection. The data shown were pooled from independent experiments, using a total of 3 mice for each date. The results are compared to those obtained in uninfected (day 0) mice. $^*p < 0.05$, $^{**}p < 0.01$, 2-way ANOVA with Tukey's multiple comparison test. The data are shown as the mean ± SD.

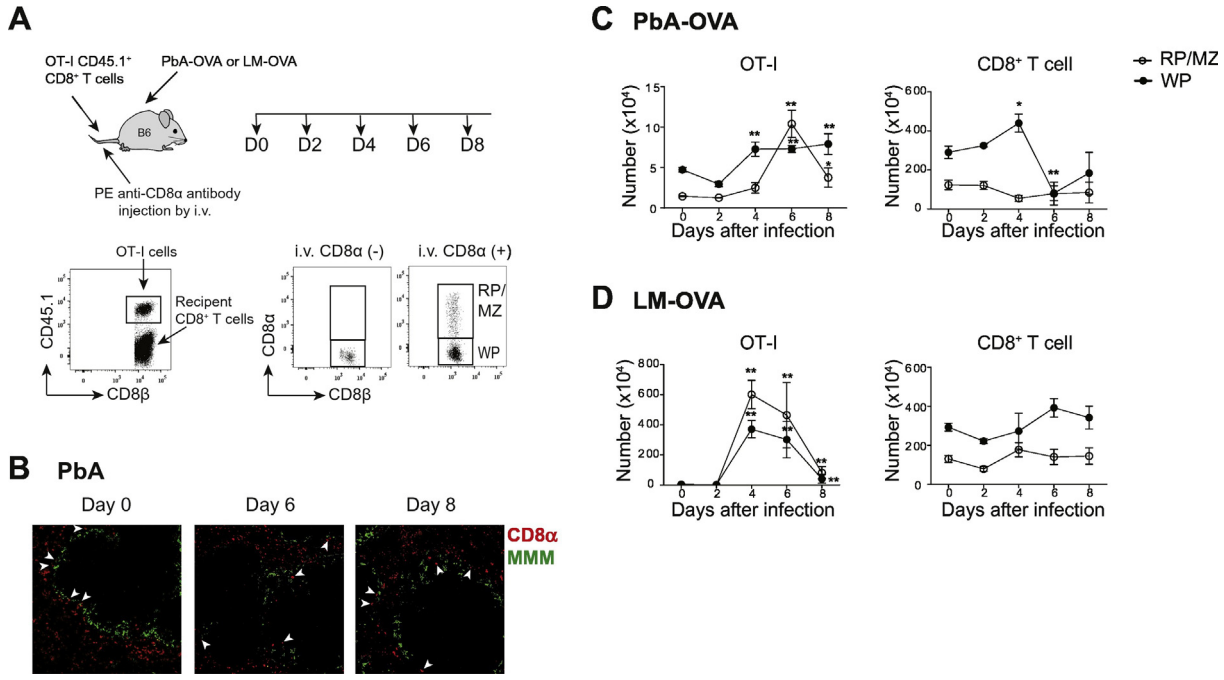

Fig. 2. Kinetics of OT-I cells in the spleens of mice infected with PbA-OVA or LM-OVA. (A) Schematic representation of the experimental design and gating strategy. C57BL/6 mice were adoptively transferred with OT-I cells and infected with PbA-OVA (C) or LM-OVA (D). Mice received PE-*anti*-CD8α mAb 3 min prior to euthanasia. The spleen cells were stained for CD45.1 and CD8β, and were analyzed by flow cytometry. (B) Spleen sections from mice infected with PbA for 0, 6, or 8 days were stained for CD169 (for MMMs). Red cells were stained with the injected PE-*anti*-CD8α mAb. Arrowheads show $CD8^+$ T cells in the MZ. (C, D) Numbers of OT-I cells ($CD45.1^+CD8\beta^+$, left panels) and host $CD8^+$ T cells ($CD45.1^-CD8\beta^+$, right panels) in the spleen compartments 0–8 days after infection with PbA-OVA (C) or LM-OVA (D). The data shown represent 2 independent experiments with 6 mice in each group. The results are compared to those of uninfected (day 0) mice. $^*p < 0.05$, $^{**}p < 0.01$, 2-way ANOVA with Tukey's multiple-comparison test. The data are shown as the mean ± SD.

OT-I cells and recipient $CD8^+$ T cells (thereafter referred to as host $CD8^+$ T cells) in the WP were 73.1 ± 4.7% and 68.7 ± 1.8%, respectively. The number of OT-I cells in the WP of uninfected mice ($4.7 \pm 0.3 \times 10^4$) increased to $7.3 \pm 0.8 \times 10^4$ in the WP of infected mice at 4 days post-infection with PbA-OVA and remained at similar levels thereafter (Fig. 2C, left). In contrast, the number of OT-I cells in the RP/MZ increased by approximately 7-fold from $1.5 \pm 0.1 \times 10^4$ in uninfected mice to $1.0 \pm 0.2 \times 10^5$ at day 6 post-infection and then decreased to $3.8 \pm 1.2 \times 10^4$ at 8 days post-infection. The number of host $CD8^+$ T cells increased at 4 days after infection and then decreased on day 6 in the WP (Fig. 2C, right). This reduction in the number of $CD8^+$ T cells in the WP was confirmed by immunohistochemical staining of the tissue sections (data not shown). At 4 days post-infection with LM-OVA, the number of OT-I cells increased 400-fold to $6.0 \pm 0.9 \times 10^6$ in the RP/MZ and to $3.7 \pm 0.6 \times 10^6$ in the WP, after which they gradually decreased in both compartments (Fig. 2D, left). The number of host $CD8^+$ T cells in the WP reached a maximum at 6 days after infection, and host $CD8^+$ T cells in the WP remained high over the LM-OVA infection period (Fig. 2D, right). Taken together, these data suggested that infection with PbA-OVA was characterized by an initial increase of OT-I cells in the WP, followed by an increase of OT-I cells and a reduction of host $CD8^+$ T cells in the RP/MZ at 6 days after infection.

3.2. OT-I cells initiated proliferation in the WP upon infection with PbA-OVA and LM-OVA

We questioned whether OT-I cells were primed and expanded in the WP or RP/MZ during infection with PbA-OVA. To monitor the proliferation of OT-I cells, C57BL/6 mice were adoptively transferred with 5-(and 6)-carboxyfluorescein diacetate succinimidyl ester (CFSE)-labeled OT-I cells and were left uninfected or infected with PbA-OVA or LM-OVA (Fig. 3A, E). OT-I cells started to proliferate as early as 2 days after infection with PbA-OVA in the WP (2.4% of OT-I cells). On days 3–4 after infection, the proportions of OT-I cells in the RP/MZ that proliferated >5 times vs. 1–5 times was similar, while the proportion in the WP that proliferated >5 times was lower, suggesting that OT-I cells initially proliferated mainly in the WP and then moved to the RP/MZ (Fig. 3A). In mice infected with LM-OVA, the percentages of OT-I cells that divided 1–5 times were 44.3% and 91.5% in the RP/MZ and WP, respectively, on day 2. These data were consistent with previous findings showing that specific $CD8^+$ T cells were primed and started to proliferate in the WP, after which they moved to the RP during Listeria infection (Fig. 3E) [20]. We also examined the expression of early activation markers on OT-I cells underdoing proliferation in the spleen. Three days after infection with PbA-OVA, approximately 40% and 15% of proliferating OT-I cells expressed CD25 or CD69, respectively, in both the RP/MZ and WP, and those proportions increased 4 days after infection (Supporting information Fig. 1A). However, the majority of proliferating OT-I cells expressed CD25 at 2 days post-infection with LM-OVA (Supporting information Fig. 1B). These data suggested that OT-I cells undergoing antigen-specific activation in the spleen of mice infected with PbA-OVA were more heterogeneous than those infected with LM-OVA.

3.3. Effector cells preferentially located in the RP/MZ in mice infected with PbA-OVA or LM-OVA

The phenotypes of OT-I and host $CD8^+$ T cells were analyzed after infection with PbA-OVA or LM-OVA. Four days after infection with PbA-OVA, most OT-I cells in both the RP/MZ and WP expressed CD25 and CD69 (Fig. 3B, Supporting information Fig. 2A). On the same day, the proportions of OT-I and host $CD8^+$ T cells exhibiting the $CD62L^{lo}CD44^{hi}$ effector phenotype were higher in the RP/MZ than in the WP (Fig. 3C, Supporting information Fig. 2B). Six days after infection with PbA-OVA, the proportions of $CD25^+$ and $CD69^+$ OT-I cells decreased, and the frequencies of OT-I cells exhibiting the $KLRG1^{hi}CD127^{lo}$ short-lived effector cell (SLEC) phenotype increased preferentially in the RP/MZ (Fig. 3D, Supporting information Fig. 2C). Changes in these phenotypes were mostly antigen-specific, as they were not observed in mice

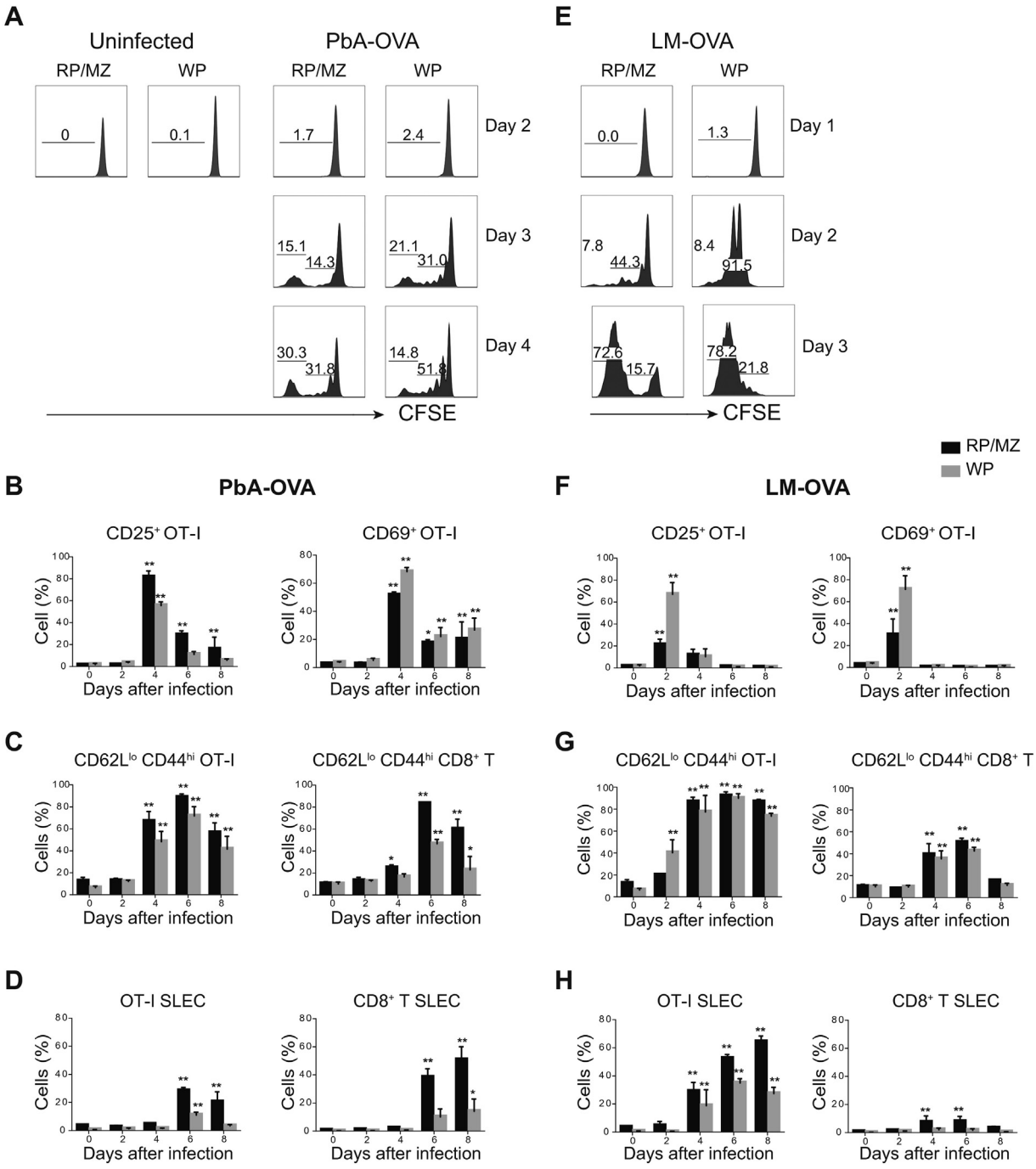

Fig. 3. OT-I cells proliferated in the WP and effector cells preferentially localized in the RP/MZ of the spleen in mice infected with PbA-OVA or LM-OVA. (A, E) C57BL/6 mice were adoptively transferred with CFSE-labeled OT-I cells and uninfected or infected with PbA-OVA (A) or LM-OVA (E). Mice received PE-*anti*-CD8α mAb prior to euthanasia, and the spleen cells were stained for CD45.1 and CD8β. CFSE profiles of OT-I cells in the RP/MZ ($CD45.1^+CD8\alpha^+CD8\beta^+$) or the WP ($CD45.1^+CD8\alpha^-CD8\beta^+$) of mice infected with PbA-OVA (A) or LM-OVA (E). The numbers shown indicate the proportions (%) of cells under the line. The data shown represent 2 experiments, with 2 mice in each group. (B–D, F–H) C57BL/6 mice were adoptively transferred with OT-I cells and infected with PbA-OVA (B–D) or LM-OVA (F–H), with uninfected (day 0) mice serving as controls. Mice received i.v. injection of PE-*anti*-CD8α mAb prior to euthanasia to determine the localization of OT-I ($CD45.1^+$) and host $CD8^+$ T ($CD45.1^-$) cells in the RP/MZ (black bar) and WP (gray bar), and the spleen cells were stained for CD45.1/CD8β and CD25/CD69 (B, F), CD44/CD62L (C, G), or KLRG1/CD127 (D, H). The data shown represent 2 independent experiments, with 6 mice in each group. The results are compared to those obtained with uninfected (day 0) mice. $^*p < 0.05$, $^{**}p < 0.01$, 2-way ANOVA with Tukey's multiple comparison test. The data are shown as the mean ± SD.

infected with PbA (Supporting information Fig. 3). Interestingly, on day 6 of the PbA-OVA infection, most host $CD8^+$ T cells in both the RP/MZ and WP presented with the $CD62L^{lo}CD44^{hi}$ effector phenotype, suggesting that they were activated in either an antigen-specific or antigen-non-specific manner. These data suggested that activated OT-I cells and host $CD8^+$ T cells mostly moved to the RP/MZ where they terminally differentiated into effector cells during PbA-OVA infection. Activation of OT-I cells during LM-OVA infection occurred approximately 2 days earlier and was stronger than that observed during PbA-OVA infection. Two days after infection with LM-OVA, the proportion of $CD25^+$ and $CD69^+$ OT-I cells increased mainly in the WP (Fig. 3F), and the proportion of the effector-phenotype OT-I cells increased in the WP (Fig. 3G). Four days after infection, the frequencies of effector OT-I and host $CD8^+$ T cells increased in both the RP/MZ and WP (Fig. 3G). The

proportion of host CD8$^+$ T cells exhibiting the SLEC phenotype did not increase in mice infected with LM-OVA, although this phenotype became a major population during infection with PbA-OVA (Fig. 3H, Supporting information Fig. 2C).

3.4. The ability of CD8$^+$ T cells to produce cytokines is reduced during PbA-OVA infection

We next measured the ability of OT-I cells to produce IFN-γ, TNF-α, and granzyme B in response to $OVA_{257–264}$ by intracellular staining (Fig. 4). The frequency of IFN-γ, TNF-α, and granzyme B-producing OT-I cells peaked on day 6 after infection with PbA-OVA and then decreased on day 8 (Fig. 4A, B; Supporting information Fig. 4A, B). The proportions of cells were always higher in the RP/MZ than in the WP. OT-I cells showed a prompt response and sustained an increase in IFN-γ production in both the RP/MZ and WP in LM-OVA-infected mice, and the overall frequency was almost 2 times higher compared with that in PbA-OVA-infected mice. The proportion of OT-I cells producing both IFN-γ and TNF-α also increased from day 3 to 8 of the infection in both the RP/MZ and WP (Fig. 4C, Supporting information Fig. 4C). However, the frequency of granzyme B$^+$ OT-I cells was highest 3 days after infection with LM-OVA and then decreased in both the RP/MZ and WP (Fig. 4D, Supporting information Fig. 4D).

3.5. OT-I cells in the RP/MZ express inhibitory receptors during infection with PbA-OVA

To determine the mechanism underlying the reduction of cytokine-producing OT-I cells during PbA-OVA infection, we examined apoptosis and expression of the inhibitory molecules PD-1, LAG-3, and TIM-3 in CD8$^+$ T cells. In PbA-OVA-infected mice, OT-I cells in the RP/MZ preferentially expressed these inhibitory molecules on their surfaces as early as 4 days after infection and the expression levels increased towards 8 days after infection (Fig. 5A, Supporting information Fig. 5A). The expression of these molecules was antigen-specific, as the expression was barely detectable in OT-I cells in mice infected with PbA (Supporting information Fig. 3). Host CD8$^+$ T cells in the RP/MZ of the infected mice expressed the inhibitory molecules on day 6 of the infection. They were exclusively expressed on CD11a^{hi} activated CD8$^+$ T cells, which represented 51.1% of the CD8$^+$ T cells in the RP/MZ 6 days after infection (data not shown). In contrast, OT-I cells expressed these inhibitory molecules transiently on day 2 during infection with LM-OVA, and their levels were higher in OT-I cells located in the WP than those in the RP/MZ (Fig. 5C, Supporting information Fig. 5C). We did not detect significant expression of these molecules on host CD8$^+$ T cells during LM-OVA infection.

We also examined apoptosis of OT-I and host CD8$^+$ T cells by staining for annexin V and 7-AAD, as the number of OT-I and host CD8$^+$ T cells dropped on day 8 and 6 of infection with PbA-OVA, respectively (Fig. 1). The proportions of apoptotic, annexin V$^+$7-AAD$^-$ OT-I or CD8$^+$ T cells increased in the RP/MZ, but not in the WP, at 4 days after infection with PbA-OVA compared to those in naïve mice (Fig. 5B, Supporting information Fig. 5B). Upon LM-OVA infection, the proportion of apoptotic OT-I or CD8$^+$ T cells reached a maximum 2 days after infection in the RP/MZ and declined thereafter (Fig. 5D, Supporting information Fig. 5D). Similar to PbA-OVA infection, few OT-I and host CD8$^+$ T cells in the WP underwent apoptosis over the period of LM-OVA infection except on day 2. These results suggested that OT-I cells express inhibitory receptors predominantly in the RP/MZ, leading to their exhaustion and apoptosis during PbA-OVA infection.

4. Discussion

We investigated CD8$^+$ T-cell activation kinetics in the splenic tissue of mice infected with PbA-OVA and in antigen-specific CD8$^+$ OT-I cells in comparison with those of mice infected with LM-OVA. Our data showed that OT-I cells increased in the WP prior to increasing in the RP/MZ after infection with PbA-OVA in a manner similar to that in mice infected with LM-OVA. Studying T cell proliferation using CFSE also showed that OT-I cells started to proliferate in the WP after infection with PbA-OVA or LM-OVA. OT-I cells appearing in the RP/MZ during the early period of PbA-OVA infection proliferated and expressed effector phenotypes, while a large proportion of OT-I cells in the WP proliferated <5 times, suggesting that most OT-I cells proliferated in the WP and then moved to RP/MZ, although some OT-I cells may have also proliferated in the RP/MZ. OT-I cells in RP/MZ produced IFN-γ, TNF-α, and

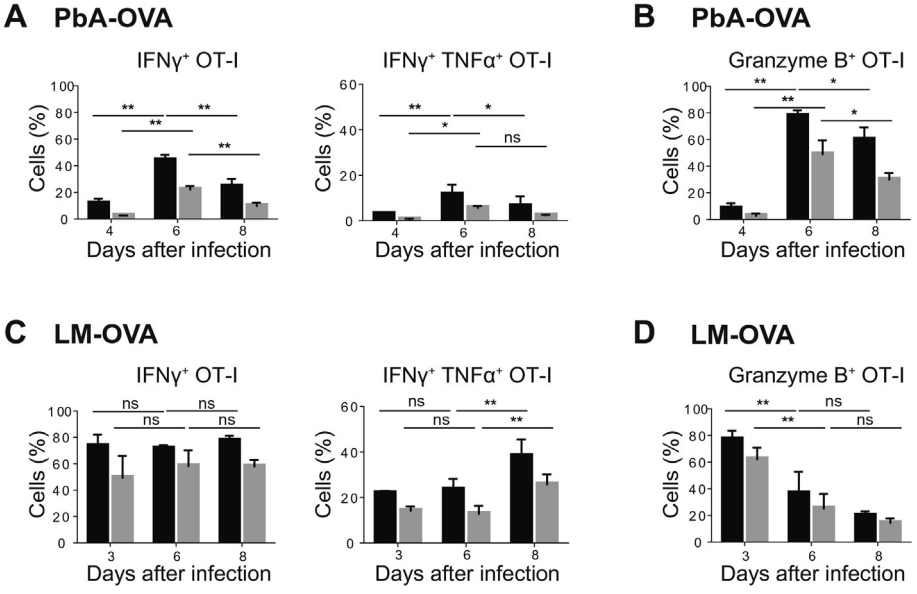

Fig. 4. Cytokine production was reduced in OT-I cells after prolonged infection with PbA-OVA. C57BL/6 mice were adoptively transferred with OT-I (CD45.1$^+$) cells and infected with PbA-OVA (A, B) or LM-OVA (C, D). Mice received i.v. injection of PE-*anti*-CD8α mAb prior to euthanasia. After intracellular staining, the proportions of IFN-γ$^+$, IFN-γ$^+$TNF-α$^+$ (A, C), and granzyme B$^+$ (B, D) OT-I cells within the total OT-I cell population in the RP/MZ (black bar) and WP (gray bar) were determined. The data shown are from 2 experiments with 4–6 mice in each group. Results from day 4 vs. day 6, and day 6 vs. day 8 in each compartment are compared (A, B). Results from day 3 vs. day 6, and day 6 vs. day 8 in each compartment are compared (C, D). *$p < 0.05$, **$p < 0.01$, ns $p > 0.05$, 2-way ANOVA with Tukey's multiple comparison test. The data are shown as the mean ± SD.

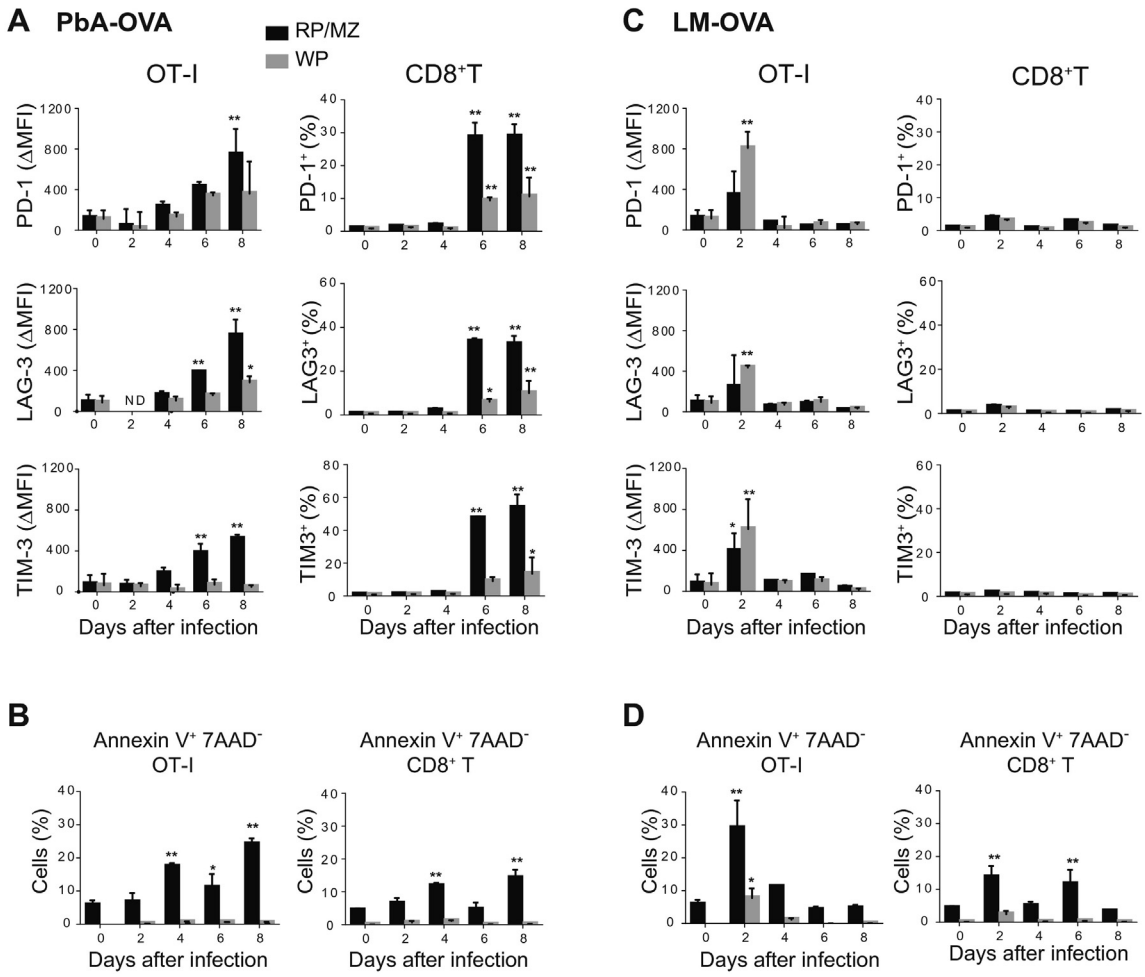

Fig. 5. CD8$^+$ T cells in the RP/MZ preferentially expressed inhibitory receptors during PbA-OVA infection. B6 mice were adoptively transferred with OT-I (CD45.1$^+$) cells and infected with PbA-OVA (A, B) or LM-OVA (C, D). Mice received i.v. injection of PE-*anti*-CD8α mAb prior to euthanasia, and the spleen cells were stained for CD45.1, CD8β, PD-1, LAG-3, and TIM-3 (A, C), or stained for CD45.1, CD8β, Annexin V, and 7AAD (B, D). Differences in MFIs observed between OT-1 cells stained with an antigen-specific antibody vs. an isotype control (ΔMFI; left) and the proportions (%) of cells expressing inhibitory receptors on host CD8$^+$ T cells (right) in the RP/MZ (black bars) and WP (gray bars) were determined. ND; not detected. The proportions (%) of apoptotic (annexin V$^+$7AAD$^-$) OT-I cells (upper) and host CD8$^+$ T cells (lower) located in the RP/MZ (black bars) and WP (gray bars) were determined. Two independent experiments with 6 mice in each group were performed. The results are compared to those obtained in uninfected (day 0) mice. $^*p < 0.05$, $^{**}p < 0.01$, 2-way ANOVA with Tukey's multiple comparison test. The data are shown as the mean ± SD.

granzyme B in response to TCR stimulation, at least during the early period of PbA-OVA infection. These features suggested that *Plasmodium*-specific CD8$^+$ T cells were initially primed in the WP of the spleen similar to that observed in Listeria and viral infections [20–23]. Because *Plasmodium* parasites infect RBCs, which are abundant in the RP, *Plasmodium* antigens in the RP may be carried to the WP by DCs and presented to CD8$^+$ T cells in the T cell zone of the WP.

During PbA-OVA infection, we observed several features of OT-I cell activation that differed from those observed during LM-OVA infection. The activation of OT-I cells was less robust during PbA-OVA infection, perhaps reflecting the slower growth of *Plasmodium* parasites as well as their sequestration in RBCs when compared with Listeria. In addition, the activation of OT-I cells progressed in a more heterogeneous manner during PbA-OVA infection in terms of the number of divisions and the expression of activation markers. Because parasitemia increased gradually during PbA-OVA infection, presentation of *Plasmodium* antigens might have occurred via a small number of DCs, which increased in parallel with the increase in parasitemia. Furthermore, the cell types that presented microbial antigens to CD8$^+$ T cells were likely different during malaria and Listeria infection. During infection with *L. monocytogenes*, CD8α$^+$ DCs are infected with microbes and carry their antigens to the T cell zone in the WP, where they present microbial antigens to CD8$^+$ T cells [17–19], while DCs are not usually infected with malaria parasites. In addition, both the proportion of DC subsets and the capacity of DCs to present malarial antigens to T cells were altered during infection with *Plasmodium* parasites [32].

The most prominent difference in OT-I responses between infection with PbA-OVA and LM-OVA was that the former expressed inhibitory receptors, as reported previously [9,11,33]. During PbA-OVA infection, OT-I cells expressed PD-1, LAG-3, and TIM-3, and their expression levels were particularly high in the RP/MZ, suggesting that these molecules were expressed on CD8$^+$ T cells in the late phase of activation and cell division. The expression of these inhibitory receptors was upregulated in host CD8$^+$ T cells in a more pronounced manner in the RP/MZ after 6 days of infection with PbA-OVA. However, during LM-OVA infection, these inhibitory receptors were expressed transiently on OT-I cells, which were localized mainly to the WP on day 2 of infection, and were downregulated after a brief period. In addition, the expression of these molecules was barely observed on host-activated CD8$^+$ T cells during LM-OVA infection. These features suggested that the major tissue compartment in which specific CD8$^+$ T cells express inhibitory receptors during infection with malaria parasites was the RP/MZ. Local phagocytic cells such as RP macrophages might be involved in the expression of inhibitory receptors by presenting parasite antigens to T cells in the RP. Continuous stimulation of activated T cells with persistent antigens in the RP during malaria infection might sustain

expression of inhibitory receptors leading to their exhaustion, as suggested for chronic viral infection [34]. Moreover, cells in the RP and MZ (such as MZMs, MMMs, and RP macrophages) may express high levels of PD-1 ligands, as previously shown during chronic viral infection [35]. In addition, malaria infection provides a unique inflammatory environment in the spleen. Hemozoin, a detoxification product of the heme molecule, accumulates during infection and promotes stimulation of immune cells such as dendritic cells and macrophages in the spleen [36]. Tr27 cells are unique regulatory $CD4^+$ T cells that produce IL-27 and are induced during *Plasmodium* infection [33]. These immune cells may directly or indirectly affect the induction of exhaustive phenotypes in $CD8^+$ T cells. We speculate that OT-I cells, which express inhibitory receptors, in RP/MZ eventually undergo apoptosis, as OT-I cell apoptosis remained high in the RP/MZ during days 4–8 of PbA-OVA infection. While high levels of apoptosis were previously reported in the spleens of malaria-infected mice, tissue localization was not clearly investigated [37]. Our data suggest that apoptosis of specific $CD8^+$ T cells occurred mainly in the RP and MZ. In contrast, an increase in apoptotic OT-I cells was detected only on day 2 after LM-OVA infection. Taken together, these data indicated that OT-I cells were activated in a similar manner by infection with either PbA-OVA or LM-OVA, mainly in the WP of the spleen, but the fate of these OT-I cells differed. OT-I cells expressed inhibitory receptors leading to their exhaustion and apoptosis in the RP/MZ during infection with PbA-OVA, while OT-I cells maintained their activity and became memory cells after clearance of LM-OVA.

Another unique feature of malaria infection was the severe reduction of host $CD8^+$ T cells in the WP 6 days after infection with PbA-OVA. This reduction was unique to $CD8^+$ T cells and was not observed in $CD4^+$ T cells or B cells in the WP (data not shown). It is unlikely that this reduction resulted from apoptosis of $CD8^+$ T cells in the WP because we did not observe increased apoptosis of $CD8^+$ T cells 6 days after infection with PbA-OVA. In contrast, the proportion of OT-I cells in the RP/MZ greatly increased on the same day, suggesting that malaria-specific $CD8^+$ T cells were activated and moved from the WP to the RP/MZ. Therefore, we think that it is likely that the reduction was due to the movement of $CD8^+$ T cells out of the WP, although the number of host $CD8^+$ T cells did not increase in the RP/MZ. In agreement, the majority of $CD8^+$ T cells in the RP/MZ on day 6 of PbA-OVA infection presented an effector phenotype. The discrepancy of the cellular kinetics observed between OT-I cells and host $CD8^+$ T cells may involve multiple factors, including the affinity of the TCR for *Plasmodium*-antigen or, antigen-independent activation of $CD8^+$ T cells as previously suggested [6]. Further study is required to resolve this question.

Studies of OT-I function showed that expression of granzyme B was relatively maintained, while cytokine production was reduced in the later phase of PbA-OVA infection, which is consistent with our previous study [6]. These results suggested that the cytotoxic ability and cytokine production of $CD8^+$ T cells may be differentially regulated in $CD8^+$ T cells. Excess activation of cytotoxicity in specific $CD8^+$ T cells facing increased antigenic load in parallel to the parasitemia may lead to pathogenic effects in the host tissue, resulting in destruction of the splenic tissue architecture, including MMMs [26]. In contrast, the production of granzyme B decreased in the later phase of LM-OVA infection when the microbial burden was reduced, reducing damage to the host tissue.

In conclusion, we present evidence suggesting that the activation and expression of inhibitory receptors, leading to exhaustion of $CD8^+$ T cells, are likely to occur in distinct compartments in the spleen (the WP and RP, respectively). While the RP has been considered as a blood-filtering system [12], our findings suggest that the RP serves additional roles in regulating immune responses, in particular during malaria infection. One caveat is that this study was performed using a model antigen, and further investigation is required to confirm these findings in natural settings. Despite such limitations, the role of the RP in immune responses was particularly highlighted in malaria infection, as the RP is the tissue where antigens are concentrated. The mechanisms underlying the induction and maintenance of exhausted T cells are critical in generating effective protective immunity against malaria. Further study will reveal these mechanisms in addition to their localization in the RP/MZ, leading to novel diagnostic and therapeutic strategies for chronic infectious diseases, including malaria, in the future.

Funding

This work was supported by Grants-in-Aid from the Ministry of Education, Science, Sports and Culture, Japan to M.M. (23590487) and K. Yui (24659189, 25293101). The funding source was not involved in any part of the study design, analysis, or interpretation of the data.

Conflict of interest disclosure

The authors declare no commercial or financial conflict of interest.

Acknowledgements

We thank Dr. H. Kosaka for providing mice; Drs. Y. Yoshikai and H. Shen for providing LM-OVA; and K. Kimura and N. Kawamoto for providing technical assistance. We also thank Dr. W. Heath (Univ. Melbourne, Australia) for allowing G.B. to perform a part of the study in his laboratory. We would like to thank Editage for English language editing.

Appendix A. Supplementary data

Supplementary data to this article can be found online at http://dx.doi.org/10.1016/j.parint.2017.01.022.

References

[1] WHO, World Malaria Report (2015) 2015.
[2] M.F. Good, H. Xu, M. Wykes, C.R. Engwerda, Development and regulation of cell-mediated immune responses to the blood stages of malaria: Implications for vaccine research, Annu. Rev. Immunol. 23 (2005) 69–99.
[3] J. Langhorne, F.M. Ndungu, A.M. Sponaas, K. Marsh, Immunity to malaria: more questions than answers, Nat. Immunol. 9 (7) (2008) 725–732.
[4] E. Belnoue, M. Kayibanda, A.M. Vigario, J.C. Deschemin, N. van Rooijen, M. Viguier, et al., On the pathogenic role of brain-sequestered αβ $CD8^+$ T cells in experimental cerebral malaria, J. Immunol. 169 (11) (2002) 6369–6375.
[5] L. Schofield, G.E. Grau, Immunological processes in malaria pathogenesis, Nat. Rev. Immunol. 5 (9) (2005) 722–735.
[6] M. Miyakoda, D. Kimura, M. Yuda, Y. Chinzei, Y. Shibata, K. Honma, et al., Malaria-specific and nonspecific activation of $CD8^+$ T cells during blood stage of *Plasmodium berghei* infection, J. Immunol. 181 (2) (2008) 1420–1428.
[7] R.J. Lundie, T.F. de Koning-Ward, G.M. Davey, C.Q. Nie, D.S. Hansen, L.S. Lau, et al., Blood-stage *Plasmodium* infection induces $CD8^+$ T lymphocytes to parasite-expressed antigens, largely regulated by $CD8\alpha^+$ dendritic cells, Proc. Natl. Acad. Sci. U. S. A. 105 (38) (2008) 14509–14514.
[8] T. Imai, J. Shen, B. Chou, X. Duan, L. Tu, K. Tetsutani, et al., Involvement of $CD8^+$ T cells in protective immunity against murine blood-stage infection with *Plasmodium yoelii* 17XL strain, Eur. J. Immunol. 40 (4) (2010) 1053–1061.
[9] N.S. Butler, J. Moebius, L.L. Pewe, B. Traore, O.K. Doumbo, L.T. Tygrett, et al., Therapeutic blockade of PD-L1 and LAG-3 rapidly clears established blood-stage *Plasmodium* infection, Nat. Immunol. 13 (2) (2012) 188–195.
[10] J.M. Horne-Debets, R. Faleiro, D.S. Karunarathne, X.Q. Liu, K.E. Lineburg, C.M. Poh, et al., PD-1 dependent exhaustion of $CD8^+$ T cells drives chronic malaria, Cell Rep. 5 (5) (2013) 1204–1213.
[11] J.C. Hafalla, C. Claser, K.N. Couper, G.E. Grau, L. Renia, J.B. de Souza, et al., The CTLA-4 and PD-1/PD-L1 inhibitory pathways independently regulate host resistance to *Plasmodium*-induced acute immune pathology, PLoS Pathog. 8 (2) (2012), e1002504.
[12] R.E. Mebius, G. Kraal, Structure and function of the spleen, Nat. Rev. Immunol. 5 (8) (2005) 606–616.
[13] L. Martinez-Pomares, S. Gordon, CD169+ macrophages at the crossroads of antigen presentation, Trends Immunol. 33 (2) (2012) 66–70.
[14] P. Aichele, J. Zinke, L. Grode, R.A. Schwendener, S.H. Kaufmann, P. Seiler, Macrophages of the splenic marginal zone are essential for trapping of blood-borne particulate antigen but dispensable for induction of specific T cell responses, J. Immunol. 171 (3) (2003) 1148–1155.
[15] R.M. Steinman, M. Pack, K. Inaba, Dendritic cells in the T-cell areas of lymphoid organs, Immunol. Rev. 156 (1997) 25–37.
[16] D. Dudziak, A.O. Kamphorst, G.F. Heidkamp, V.R. Buchholz, C. Trumpfheller, S. Yamazaki, et al., Differential antigen processing by dendritic cell subsets in vivo, Science 315 (5808) (2007) 107–111.

[17] M. Neuenhahn, K.M. Kerksiek, M. Nauerth, M.H. Suhre, M. Schiemann, F.E. Gebhardt, et al., CD8α$^+$ dendritic cells are required for efficient entry of *Listeria monocytogenes* into the spleen, Immunity 25 (4) (2006) 619–630.
[18] T. Aoshi, B.H. Zinselmeyer, V. Konjufca, J.N. Lynch, X. Zhang, Y. Koide, et al., Bacterial entry to the splenic white pulp initiates antigen presentation to CD8$^+$ T cells, Immunity 29 (3) (2008) 476–486.
[19] B.T. Edelson, T.R. Bradstreet, K. Hildner, J.A. Carrero, K.E. Frederick, W. Kc, et al., CD8α$^+$ dendritic cells are an obligate cellular entry point for productive infection by *Listeria monocytogenes*, Immunity 35 (2) (2011) 236–248.
[20] K.M. Khanna, J.T. McNamara, L. Lefrancois, In situ imaging of the endogenous CD8 T cell response to infection, Science 318 (5847) (2007) 116–120.
[21] C. Potsch, D. Vohringer, H. Pircher, Distinct migration patterns of naive and effector CD8 T cells in the spleen: correlation with CCR7 receptor expression and chemokine reactivity, Eur. J. Immunol. 29 (11) (1999) 3562–3570.
[22] J.G. Dauner, I.R. Williams, J. Jacob, Differential microenvironment localization of effector and memory CD8 T cells, J. Immunol. 180 (1) (2008) 291–299.
[23] Y.W. Jung, R.L. Rutishauser, N.S. Joshi, A.M. Haberman, S.M. Kaech, Differential localization of effector and memory CD8 T cell subsets in lymphoid organs during acute viral infection, J. Immunol. 185 (9) (2010) 5315–5325.
[24] H. Helmby, G. Jonsson, M. Troye-Blomberg, Cellular changes and apoptosis in the spleens and peripheral blood of mice infected with blood-stage *Plasmodium chabaudi* chabaudi AS, Infect. Immun. 68 (3) (2000) 1485–1490.
[25] A. Chandele, P. Mukerjee, G. Das, R. Ahmed, V.S. Chauhan, Phenotypic and functional profiling of malaria-induced CD8 and CD4 T cells during blood-stage infection with *Plasmodium yoelii*, Immunology 132 (2) (2011) 273–286.
[26] L. Beattie, C.R. Engwerda, M. Wykes, M.F. Good, CD8$^+$ T lymphocyte-mediated loss of marginal metallophilic macrophages following infection with *Plasmodium chabaudi* chabaudi AS, J. Immunol. 177 (4) (2006) 2518–2526.
[27] K.A. Hogquist, S.C. Jameson, W.R. Heath, J.L. Howard, M.J. Bevan, F.R. Carbone, T cell receptor antagonist peptides induce positive selection, Cell 76 (1) (1994) 17–27.
[28] R. Dudani, Y. Chapdelaine, H. Faassen Hv, D.K. Smith, H. Shen, L. Krishnan, et al., Multiple mechanisms compensate to enhance tumor-protective CD8$^+$ T cell response in the long-term despite poor CD8$^+$ T cell priming initially: comparison between an acute versus a chronic intracellular bacterium expressing a model antigen, J. Immunol. 168 (11) (2002) 5737–5745.
[29] J.G. Dauner, C.P. Chappell, I.R. Williams, J. Jacob, Perfusion fixation preserves enhanced yellow fluorescent protein and other cellular markers in lymphoid tissues, J. Immunol. Methods 340 (2) (2009) 116–122.
[30] K.G. Anderson, K. Mayer-Barber, H. Sung, L. Beura, B.R. James, J.J. Taylor, et al., Intravascular staining for discrimination of vascular and tissue leukocytes, Nat. Protoc. 9 (1) (2014) 209–222.
[31] E. Muraille, R. Giannino, P. Guirnalda, I. Leiner, S. Jung, E.G. Pamer, et al., Distinct in vivo dendritic cell activation by live versus killed *Listeria monocytogenes*, Eur. J. Immunol. 35 (5) (2005) 1463–1471.
[32] A.M. Sponaas, E.T. Cadman, C. Voisine, V. Harrison, A. Boonstra, A. O'Garra, et al., Malaria infection changes the ability of splenic dendritic cell populations to stimulate antigen-specific T cells, J. Exp. Med. 203 (6) (2006) 1427–1433.
[33] D. Kimura, M. Miyakoda, K. Kimura, K. Honma, H. Hara, H. Yoshida, et al., Interleukin-27-producing CD4$^+$ T cells regulate protective immunity during malaria parasite infection, Immunity 44 (3) (2016) 672–682.
[34] E.J. Wherry, T cell exhaustion, Nat. Immunol. 12 (6) (2011) 492–499.
[35] B.H. Zinselmeyer, S. Heydari, C. Sacristan, D. Nayak, M. Cammer, J. Herz, et al., PD-1 promotes immune exhaustion by inducing antiviral T cell motility paralysis, J. Exp. Med. 210 (4) (2013) 757–774.
[36] C. Coban, K.J. Ishii, T. Kawai, H. Hemmi, S. Sato, S. Uematsu, et al., Toll-like receptor 9 mediates innate immune activation by the malaria pigment hemozoin, J. Exp. Med. 201 (1) (2005) 19–25.
[37] L. Sanchez-Torres, A. Rodriguez-Ropon, M. Aguilar-Medina, L. Favila-Castillo, Mouse splenic CD4$^+$ and CD8$^+$ T cells undergo extensive apoptosis during a *Plasmodium chabaudi* chabaudi AS infection, Parasite Immunol. 23 (12) (2001) 617–626.